

# Optical transmission properties of light propagation through Fibonacci-class ring-resonators

A. Rostami<sup>1,2,a</sup> and G. Rostami<sup>2</sup>

<sup>1</sup> Department of ECE, University of Toronto, 10 King's College Road, Toronto, M5S 3G4, Canada

<sup>2</sup> OIC Research Lab., Faculty of Electrical and Computer Engineering, Tabriz University, Tabriz 51664, Iran

Received 11 November 2004 / Received in final form 3 March 2005

Published online 21 September 2005 – © EDP Sciences, Società Italiana di Fisica, Springer-Verlag 2005

**Abstract.** An interesting topology with easy integration capability (from mask designing aspect) for optical filters using Fibonacci-class ( $FC(J, n)$ ) ring-resonators is introduced. For some special cases, analytical transfer function (Transmission Coefficient  $H_m^{(n)}$ ) is obtained and corresponding simulated result is illustrated. In this work, optical multi-band filter design and analysis using Fibonacci-class ring resonators is considered. With suitable selection of system parameters and  $FC(J, n)$ , we report multi-band characteristic for this structure. Also, dominant factors effects on multi-band operation are shown. We show that the coupling coefficients, effectively affects (e.g. generation or annihilation of additional band) the multi-band properties obtained in proposed structure. Also, the bandwidth and position of additional band can be controlled using Fibonacci-class basic elements (A, B) parameters such as rings diameters. Also, proposed system is easier than general multistage rings coupled to main waveguide from implementation point of view.

**PACS.** 41.20.Jb Electromagnetic wave propagation; radiowave propagation – 42.79.Gn Optical waveguides and couplers – 42.82.Gw Other integrated-optical elements and systems – 42.25.Bs Wave propagation, transmission and absorption

## 1 Introduction

Transport phenomena of light waves in three, two, and one-dimensional complex structures have attracted a lot of attention in the last years. Complex photonic structures are artificial materials in which the index of refraction has a particular variation on length scales comparable to the wavelength of light. A periodic variation of the refractive index gives rise to a photonic crystal structure. At high enough refractive index contrast these periodic systems can exhibit a photonic band gap, in analogy with the band gap for electron in a semiconductor. In this direction, there are many published papers and approximately main part of these properties was reported [1,2]. Also, optical integrated circuit design and implementation is very interesting subject from optical engineering purposes point of view. One of basic and critical properties for optical integrated circuits (OIC) is integration capability with usual planar technology for semiconductors. Because of inherent potentials in this domain, proposing monolithic special blocks such as signal conditioners is considerable. From all devices for signal conditioners, optical filters has basic role and is important. For example, with engineering dense wavelength division mul-

tiplexing systems (DWDM) and with increasing the number of channels in practice, we need very narrowband filters for separating single or multi channels simultaneously. For realization of these filters there are many alternatives such as fiber Bragg Gratings, which is discussed more in the reported papers and textbooks. Also, quasi-periodic structures are one of interesting cases for realization of narrowband optical filters. Quasi-periodic structures can be implemented by two methods. One of these methods is multilayer structure, which need epitaxial methods for implementation. The optical properties of Fibonacci based multilayer structures were studied in [3–6]. The second one is ring-resonators, which is presented here. So, here, ring resonator as a basic element for optical filters is considered. In this work, we will study the optical properties of Fibonacci-class ring resonators as optical filters. Also, optical ring resonators were studied more in [7–10]. From our point of view, Fibonacci-based ring-resonators arrangement needs more study and calculations. So, in this paper, we will concentrate on optical properties of light propagation through Fibonacci-class ring-resonators. Specially, in this work, we present a design for optical filters with minimum masks for manufacturing. In this idea, the only difference between rings is the radius of rings, which is simple for manufacturing. The organization of this paper is as follows.

---

<sup>a</sup> e-mail: rostami@tabrizu.ac.ir

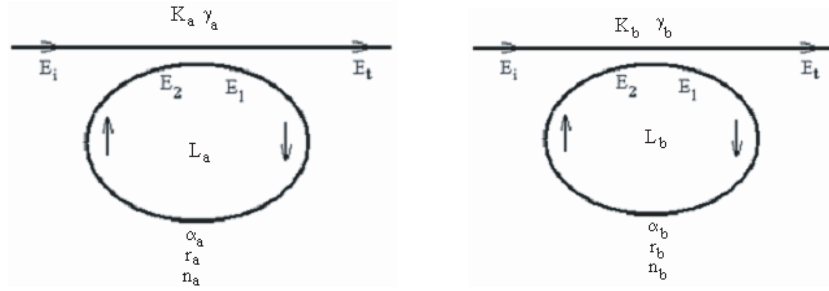


**Fig. 1.** Simple schematics of ring resonators coupled to optical waveguide (*A* and *B* corresponding to Fibonacci basic units).

In Section 2, mathematical modeling for investigating the optical behavior of proposal is presented. For this purpose, first we introduce the basic transfer function for Fibonacci elements and ring resonators coupled to main waveguide and then generalize for arbitrary arrangement of ring resonators according to Fibonacci algorithm. Results and discussion for some special cases are presented in Section 3. Finally, the paper ends with a short conclusion.

## 2 Mathematical modeling of Fibonacci-class ring-resonators

Figure 1 shows the simple schematics of ring resonators coupled to optical waveguides with ring diameter  $r_i$ , ( $i = A, B$ ), the coupling coefficient  $K_i$ , the index of refraction  $n_i$ , the incident field  $E_i$  and the outgoing field  $E_t$  for both elements of our considering Fibonacci-class. Also,  $E_1$  and  $E_2$  are output and input fields inside rings near the coupling region.

For this structure  $L_i = 2\pi r_i$ ,  $\gamma_i$ ,  $k_{ni}$  and  $\alpha_i$ , are the ring length, the coupler attenuation coefficient, the wave vector and the ring attenuation coefficient respectively for  $i = A$  and  $B$ .

In this part, we introduce the Fibonacci-class  $FC(J, n)$ . In Fibonacci sequence, we need two basic elements named *A* and *B*. Here, *A* and *B* are ring resonators and demonstrated in Figure 1. The  $FC(J, n)$  shown the Fibonacci-class sequences with index *J* as sequence character and *n* as pointer of generalized model. The  $FC(J, n)$  sequence is a class of quasi-periodic lattice generated by substitution rules as

$$B \rightarrow B^{n-1}A, A \rightarrow B^{n-1}AB, \tag{1}$$

where *n* is a positive integer number and generalized Fibonacci-class model factor. So, using equation (1), with starting from *B*, we have

$$\begin{aligned} S_1 &= B, \\ S_2 &= B^{n-1}A, \\ S_3 &= (B^{n-1}A)^n B, \end{aligned} \tag{2}$$

which follows the following recursion relation as

$$S_J = S_{J-1}^n S_{J-2}, \quad \text{for } J \geq 3. \tag{3}$$

If equation (3) expanded for  $J = 3, 4, 5$ , we obtain the following relations

$$\begin{aligned} S_3 &= S_2^n S_1 = (B^{n-1}A)^n B \\ &= (BB \dots BA)(BB \dots BA) \dots (BB \dots BA)B' \\ S_4 &= S_3^n S_2 = [(B^{n-1}A)^n B]^n (B^{n-1}A)' \\ S_5 &= S_4^2 S_3 = [[(B^{n-1}A)^n B]^n (B^{n-1}A)]^n (B^{n-1}A)^n B. \end{aligned} \tag{4}$$

So, after introducing Fibonacci sequence in terms of basic elements, we calculate the basic elements transfer functions. According to mode coupling theory and assuming single mode for main waveguide and rings, the input-output relation is given as

$$\begin{aligned} E_t &= \sqrt{1-\gamma_i} \cdot [E_i \cdot \sqrt{1-K_i} + j\sqrt{K_i} \cdot E_2], \\ E_1 &= \sqrt{1-\gamma_i} \cdot [E_2 \cdot \sqrt{1-K_i} + j\sqrt{K_i} \cdot E_{in}], \end{aligned} \tag{5}$$

where  $i = A, B$ ,  $\gamma_i$  and  $K_i$  are intensity insertion loss and the coupling factors and normalized to related overlap integrals or effective areas (determined by mode functions) and values changes from zero to one in our calculation. In fact guided mode shape will determine insertion loss and coupling factor in basic elements. The relation between  $E_1$  and  $E_2$  can be obtained based on light transmission theory in homogeneous medium as

$$E_2 = E_1 \cdot e^{-\frac{\alpha_i}{2} \cdot L_i} \cdot e^{-jk_{n_i} \cdot L_i}, \tag{6}$$

where  $k_{n_i} = \frac{2\pi}{\lambda} n_i$  is the wave vector and  $n_i$  is the rings index of refractions in Figure 1. Also,  $\alpha_i$  is ring loss (roundtrip loss), which includes propagation loss, losses from transitions in the curvature, and bending losses. Using equations (5-6), we obtain the following transfer function for Fibonacci basic elements as

$$\begin{aligned} \left. \frac{E_t}{E_{in}} \right|_i &= \\ &= \sqrt{1-\gamma_i} \cdot \left( \frac{\sqrt{1-K_i} - \sqrt{1-\gamma_i} \cdot e^{-\frac{\alpha_i}{2} L_i} \cdot e^{-jk_{n_i} L_i}}{1 - \sqrt{(1-K_i)} \cdot (1-\gamma_i) \cdot e^{-\frac{\alpha_i}{2} L_i} \cdot e^{-jk_{n_i} L_i}} \right), \end{aligned} \tag{7}$$

where,  $H_A$  and  $H_B$  are defined as

$$H_{A,B} = \left. \frac{E_t}{E_{in}} \right|_{i=A,B}.$$

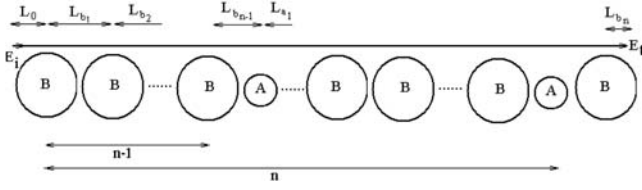


**Fig. 2.** Our Fibonacci-based proposal as optical filter for  $FC(J = 3, n)$ .

Now, our proposal for optical filtering block, for example for  $J = 3$ , is shown in Figure 2.

Now, using equations (3–4), Figure 2 and performing some mathematical calculation and manipulations on them, we obtain the following relation for system transfer function (transmission coefficient  $H_m^{(n)}$ ) as

$$H_3^{(n)} = \frac{E_t}{E_i} \Big|_{J=3,n} = e^{-\frac{\alpha_0}{2}\xi} e^{-jK_{n_0}\xi} H_B^{n(n-1)+1} H_A^n, \quad (8)$$

where

$\xi = 2nr_a + 2[n(n-1) + 1]r_b + (n^2 + 2)L$ . Also,  $n_0$  and  $\alpha_0$  are the index of refraction and propagation loss in main waveguide ( $K_{n_0}$  is wave vector in main waveguide).

Also, in the above equation,  $r_a$ ,  $r_b$  and  $L$  are the ring A, B radiuses respectively and distance between rings such that, we have,

$$\begin{aligned} L_0 &= r_b + L, \\ L_{b1} &= r_b + L + r_b, \\ &\cdot \\ &\cdot \\ L_{b_{n-1}} &= r_b + L + r_a. \end{aligned} \quad (9)$$

Also, using similar calculations the following relations is obtained for  $J = 4$  as

$$H_4^{(n)} = \frac{E_t}{E_i} \Big|_{J=4,n} = e^{-\frac{\alpha_0}{2}\eta} e^{-jK_{n_0}\eta} H_B^{(n^2+1)(n-1)+n} H_A^{n^2+1}, \quad (10)$$

where

$$\eta = 2(n^2 + 1)r_a + 2[n^3 - n^2 + 2n - 1]r_b + (n^3 + 2n + 1)L.$$

Using similar methods, we can propose the following transfer function for general case as

$$H_m^{(n)} = \frac{E_t}{E_i} \Big|_{J=m,n} = e^{-\frac{\alpha_0}{2}\chi_m} e^{-jK_{n_0}\chi_m} H_B^{f_m^{(1)}(n)} H_A^{f_m^{(2)}(n)}, \quad (11)$$

where  $\chi_m = g(r_a, r_b, L, n)$  and  $f_m^{(1,2)}(n)$  are functions of integer number  $n$ . Also,  $f_m^{(1)}(n)$  and  $f_m^{(2)}(n)$  are the number of ring B and A respectively in proposed structure. As an example, in the following table, we give the transfer functions for special cases.

Now, using many different suitable combinations for  $K_i$ ,  $\gamma_i$ ,  $\alpha_i$ ,  $k_{n_i}$ ,  $J$  and  $n$ , we can obtain excellent performances for optical filters, which are presented in the next section.

**Table 1.** Transfer coefficients for some special cases.

	$\chi_m$	$f_m^{(1)}(n)$	$f_m^{(2)}(n)$
$H_7^{(1)}$	$16r_a + 10r_b + 14L$	5	8
$H_6^{(1)}$	$10r_a + 6r_b + 8L$	3	5
$H_5^{(1)}$	$6r_a + 4r_b + 6L$	2	3
$H_4^{(1)}$	$4r_a + 2r_b + 4L$	1	2
$H_3^{(1)}$	$2r_a + 2r_b + 3L$	1	1
$H_3^{(2)}$	$4r_a + 6r_b + 6L$	3	2
$H_4^{(2)}$	$10r_a + 14r_b + 13L$	7	5
$H_3^{(3)}$	$6r_a + 14r_b + 11L$	7	3
$H_3^{(4)}$	$8r_a + 26r_b + 18L$	13	4
$H_4^{(3)}$	$20r_a + 46r_b + 34L$	23	10
$H_5^{(2)}$	$24r_a + 34r_b + 31L$	17	12

### 3 Result and discussion

In this section, we will present some suitable performance of our proposed idea in Section 2. For this purpose, we try to simulate and illustrate typical curves for demonstrating our ideas. Our simulation in this paper is divided into 4 groups as follows.

1. Simulation with general basic elements parameters;
2. Finding special parameters for multi-band operation and investigating the effect of Fibonacci-class factors  $J$  on transmission coefficient with constant  $n(n = 1)$ ;
3. Investigating the effect of generalization factor  $n$  on multi-band operation;
4. System parameters effects on transmission coefficient.

So, in the following, we present the simulated result for demonstrating the above-mentioned cases.

**Case 1.** In this case, we demonstrate the transmission coefficient for system parameters without special conditions on them. In this part, we simulate our proposed optical filter transfer function for Fibonacci-class with  $n = 1$  and  $J = 3-7$ . Result for this case is shown in Figure 3 for given parameters. With increasing class factor ( $J$ ), the bandwidth for stop band is increased and the amplitude also is decreased. Increasing the stop band is related to increasing the degree of freedom (Tab. 1), and according to control system engineering, it is acceptable. According to linear system theory, increasing the system degree of freedom or poles will decrease the system pass band and increase the stop band. Also, the decreasing of transmission coefficient amplitude is related to light coupling to the large number of rings. Increasing  $J$  will increase nonlinearly the number of rings coupled to main waveguide. So, the light coupling to rings will increase nonlinearly and finally, the transmitted light is decreased.

**Case 2.** In this part, we simulate the transmission coefficient for special system parameters in which one another additional band can be appeared. Multi-band operation is one of the necessary blocks for modern signal processing in optical communication. So, design and analysis of optical

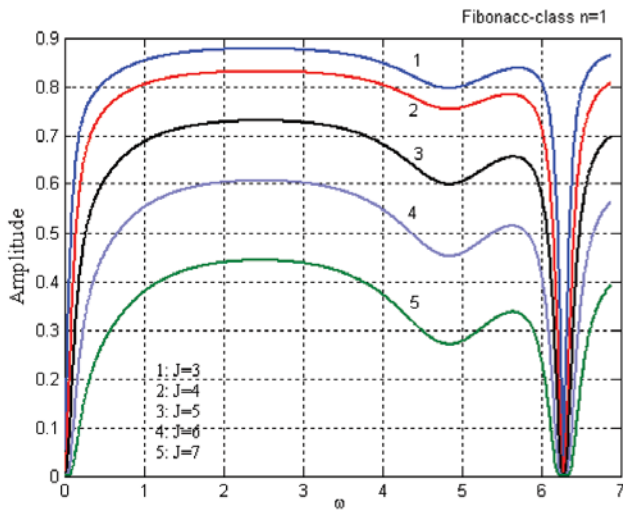
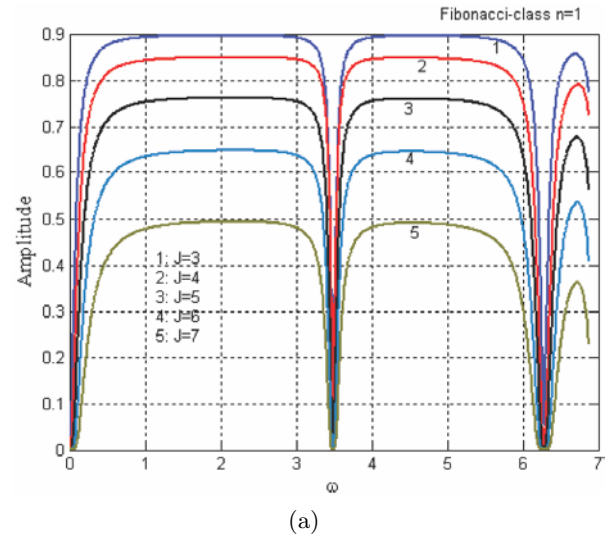


**Fig. 3.** Transmission coefficients for different  $J$  and  $n = 1$  vs. phase ( $0 - 2\pi$  for  $1.55 \mu\text{m}$ ) ( $\lambda = 1.55 \mu\text{m}$ ,  $L = 20 \mu\text{m}$ ,  $n_0 = 1.5$ ,  $\alpha_a = \alpha_b = \alpha_0 = 5 \times 10^{-5}(\mu\text{m})^{-1}$ ,  $n_a = 3$ ,  $n_b = 3$ ,  $r_a = 100 \mu\text{m}$ ,  $r_b = 130 \mu\text{m}$ ,  $\gamma_a = \gamma_b = 0.1$ ,  $k_a = 0.1$ ,  $k_b = 0.85$ ).

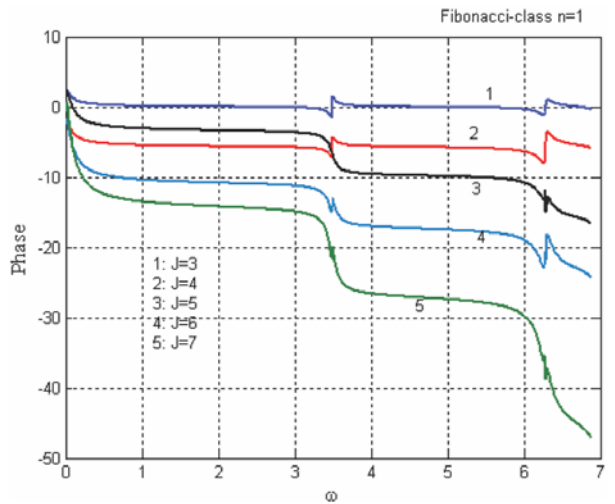
multi-band filters in this area is important. In this case, using Fibonacci-class ring resonator, we show this operation. Our simulated result is given in Figure 4a. With increasing one of the basic elements ( $B$ ) diameters, the additional band is moved from higher frequencies to lower frequencies. Also, the general behavior for increasing  $J$ , which is shown in Figure 3 for  $n = 1$ , is seen in this case. Beside, with increasing the class factor ( $J$ ), the bandwidth of additional band is increased. It is related to the increasing of power in transfer function or to the increasing of system poles. In this case, we demonstrate the phase of transmission coefficient. It is clear that in pass bands, there are linear relationships and it is excellent for signal processing purposes. Result is given in Figure 4b.

**Case 3.** In this case, we present the simulated results for demonstrating the effect of  $n$  on transmission coefficient. First, we consider the effect of  $n$  on  $J = 3$ . In Figure 5, the transmission coefficient for given parameters with different  $n$  and  $J = 3$  is illustrated. With increasing  $n$ , the bandwidth considerably increased and the amplitude is decreased. The increasing and decreasing of the bandwidth and the amplitude in this case is more than Figure 4a. This is related to nonlinear relation of  $n$  and transmission coefficient ( $H_m^{(n)}$ ). The decreasing of amplitude, generally, can be compensated using optical amplifiers in receivers. So, increasing or decreasing of  $n$  is an excellent method for bandwidth control. Also, phase relation for transmission coefficient given in Figure 5a is illustrated in Figure 5b. As previous case, there is linear relationship in pass bands.

The transmission coefficient and phase relation for  $J = 4$  and  $n = 1 - 3$  are demonstrated in Figures 5c, d. As it is shown, increasing  $n$  has critical effect for  $J = 4$  versus  $J = 3$ . As we say before, it is related to the nonlinear



(a)



(b)

**Fig. 4.** (a) Transmission coefficients for multi-band operation (for  $J = 3 - 7$  and  $n = 1$ ) vs. phase ( $0 - 2\pi$  for  $1.55 \mu\text{m}$ ) ( $\lambda = 1.55 \mu\text{m}$ ,  $L = 20 \mu\text{m}$ ,  $n_0 = 1.5$ ,  $\alpha_a = \alpha_b = \alpha_0 = 5 \times 10^{-5}(\mu\text{m})^{-1}$ ,  $n_a = 3$ ,  $n_b = 3$ ,  $r_a = 100 \mu\text{m}$ ,  $r_b = 180 \mu\text{m}$ ,  $\gamma_a = \gamma_b = 0.1$ ,  $k_a = 0.09$ ,  $k_b = 0.099$ ). (b) Phase of transmission coefficients for multi-band operation (for  $J = 3 - 7$  and  $n = 1$ ) vs. phase ( $0 - 2\pi$  for  $1.55 \mu\text{m}$ ) ( $\lambda = 1.55 \mu\text{m}$ ,  $L = 20 \mu\text{m}$ ,  $n_0 = 1.5$ ,  $\alpha_a = \alpha_b = \alpha_0 = 5 \times 10^{-5}(\mu\text{m})^{-1}$ ,  $n_a = 3$ ,  $n_b = 3$ ,  $r_a = 100 \mu\text{m}$ ,  $r_b = 180 \mu\text{m}$ ,  $\gamma_a = \gamma_b = 0.1$ ,  $k_a = 0.09$ ,  $k_b = 0.099$ ).

relation, which in case  $J = 4$  is greater than  $J = 3$ . Also, the bandwidth increasing is more than previous case.

**Case 4.** In this case, we will investigate the system parameters effects on transmission coefficient. Also, we will concentrate on  $J = 3$  and  $J = 4$  with different  $n$ . First, we show the effect of the index of refraction in rings on transmission function. Figure 6a shows the effect of basic ring- $A$  index of refraction variation on transfer function. It is shown that with decreasing the index of refraction, the additional band is moved to low frequencies approximately without broadening and amplitude changing. So,

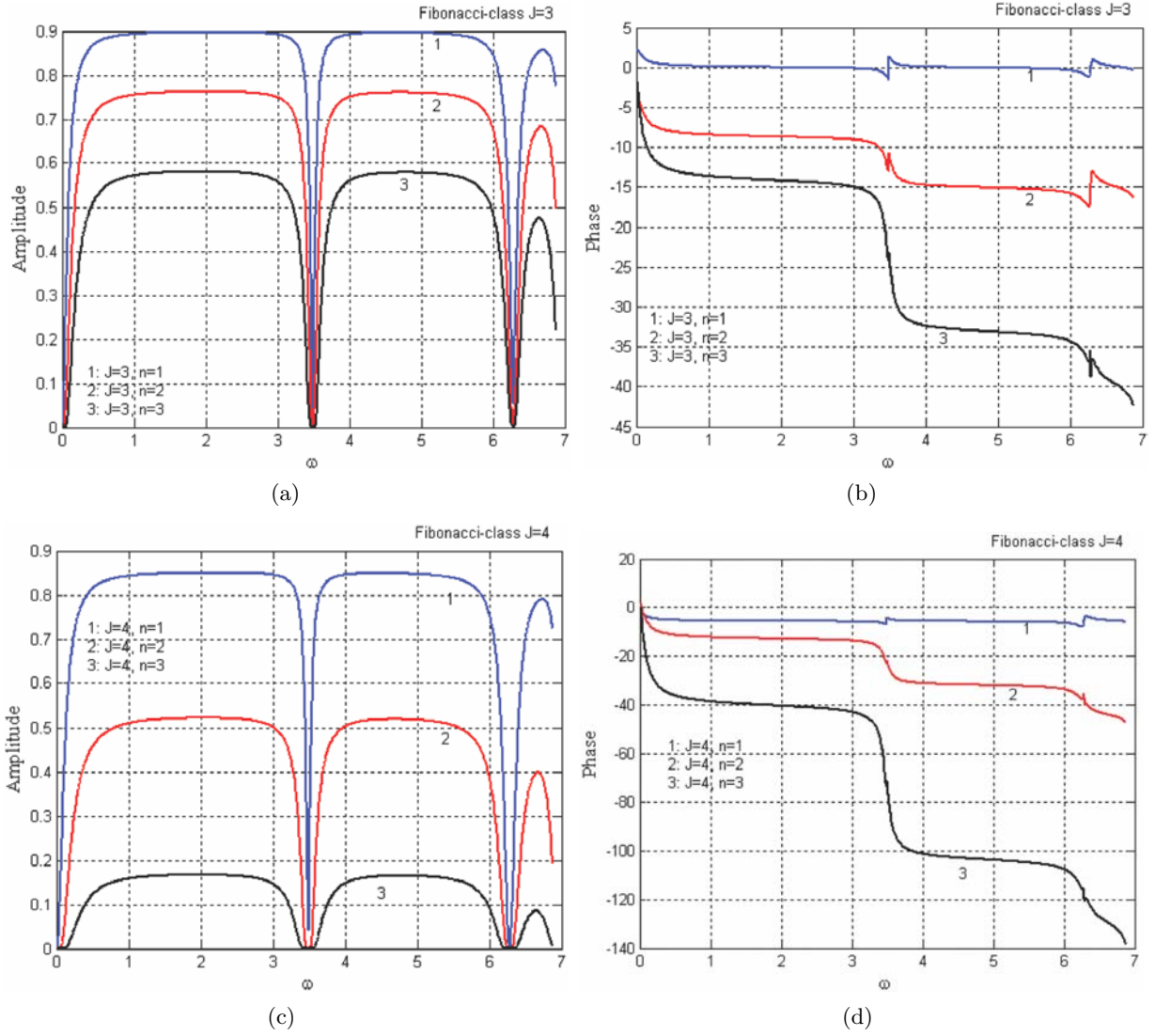


**Fig. 5.** (a) Transmission coefficients for multi-band operation (for  $J = 3$  and  $n = 1 - 3$ ) vs. phase ( $0 - 2\pi$  for  $1.55 \mu\text{m}$ ) ( $\lambda = 1.55 \mu\text{m}$ ,  $L = 20 \mu\text{m}$ ,  $n_0 = 1.5$ ,  $\alpha_a = \alpha_b = \alpha_0 = 5 \times 10^{-5}(\mu\text{m})^{-1}$ ,  $n_a = 3$ ,  $n_b = 3$ ,  $r_a = 100 \mu\text{m}$ ,  $r_b = 180 \mu\text{m}$ ,  $\gamma_a = \gamma_b = 0.1$ ,  $k_a = 0.09$ ,  $k_b = 0.099$ ). (b) Phase of transmission coefficients for multi-band operation (for  $J = 3$  and  $n = 1 - 3$ ) vs. phase ( $0 - 2\pi$  for  $1.55 \mu\text{m}$ ) ( $\lambda = 1.55 \mu\text{m}$ ,  $L = 20 \mu\text{m}$ ,  $n_0 = 1.5$ ,  $\alpha_a = \alpha_b = \alpha_0 = 5 \times 10^{-5}(\mu\text{m})^{-1}$ ,  $n_a = 3$ ,  $n_b = 3$ ,  $r_a = 100 \mu\text{m}$ ,  $r_b = 180 \mu\text{m}$ ,  $\gamma_a = \gamma_b = 0.1$ ,  $k_a = 0.09$ ,  $k_b = 0.099$ ). (c) Transmission coefficients for multi-band operation (for  $J = 3$ , and  $n = 1 - 3$ ) vs. phase ( $0 - 2\pi$  for  $1.55 \mu\text{m}$ ) ( $\lambda = 1.55 \mu\text{m}$ ,  $L = 20 \mu\text{m}$ ,  $n_0 = 1.5$ ,  $\alpha_a = \alpha_b = \alpha_0 = 5 \times 10^{-5}(\mu\text{m})^{-1}$ ,  $n_a = 3$ ,  $n_b = 3$ ,  $r_a = 100 \mu\text{m}$ ,  $r_b = 180 \mu\text{m}$ ,  $\gamma_a = \gamma_b = 0.1$ ,  $k_a = 0.09$ ,  $k_b = 0.099$ ). (d) Phase of transmission coefficients for multi-band operation (for  $J = 3$  and  $n = 1 - 3$ ) vs. phase ( $0 - 2\pi$  for  $1.55 \mu\text{m}$ ) ( $\lambda = 1.55 \mu\text{m}$ ,  $L = 20 \mu\text{m}$ ,  $n_0 = 1.5$ ,  $\alpha_a = \alpha_b = \alpha_0 = 5 \times 10^{-5}(\mu\text{m})^{-1}$ ,  $n_a = 3$ ,  $n_b = 3$ ,  $r_a = 100 \mu\text{m}$ ,  $r_b = 180 \mu\text{m}$ ,  $\gamma_a = \gamma_b = 0.1$ ,  $k_a = 0.09$ ,  $k_b = 0.099$ ).

using this result, we can fine-tune the additional band precisely. Also, similar this condition, it is for ring *B*. It is operate inversely and shift the additional band to the high frequencies, which is shown in Figure 6c. Figure 6b shows the effect of the index of refraction for ring *A* and changing  $n$  from 2 to 3 for  $J = 3$ . In this case, the similar behavior is performed with wideband additional band. In Figure 6d, we show the effect of the index of refractions variation for  $J = 4$  and  $n = 2$ . The index of refraction variation is a parameter in which its variation can only move the position of additional band. So, it is excellent factor for displacement and tuning.

In Figures 6e, f, the effect of coupling coefficient on transmission function are demonstrated. With increasing the ring-*A* coupling coefficient, we haven't any variation on the additional band, but the amplitude in pass band is distorted. But, for ring-*B*, with increasing the coupling factor, the additional band is disappeared. So, the ring *B* coupling factor can be used for managing additional band. For example for  $J = 4$ ,  $n = 2$  and  $k_b = 0.99$ , really the additional band is rejected and only common behavior is shown. Also, increasing the coupling factor will increase the trapped light in ring and finally the transmitted signal is decreased.

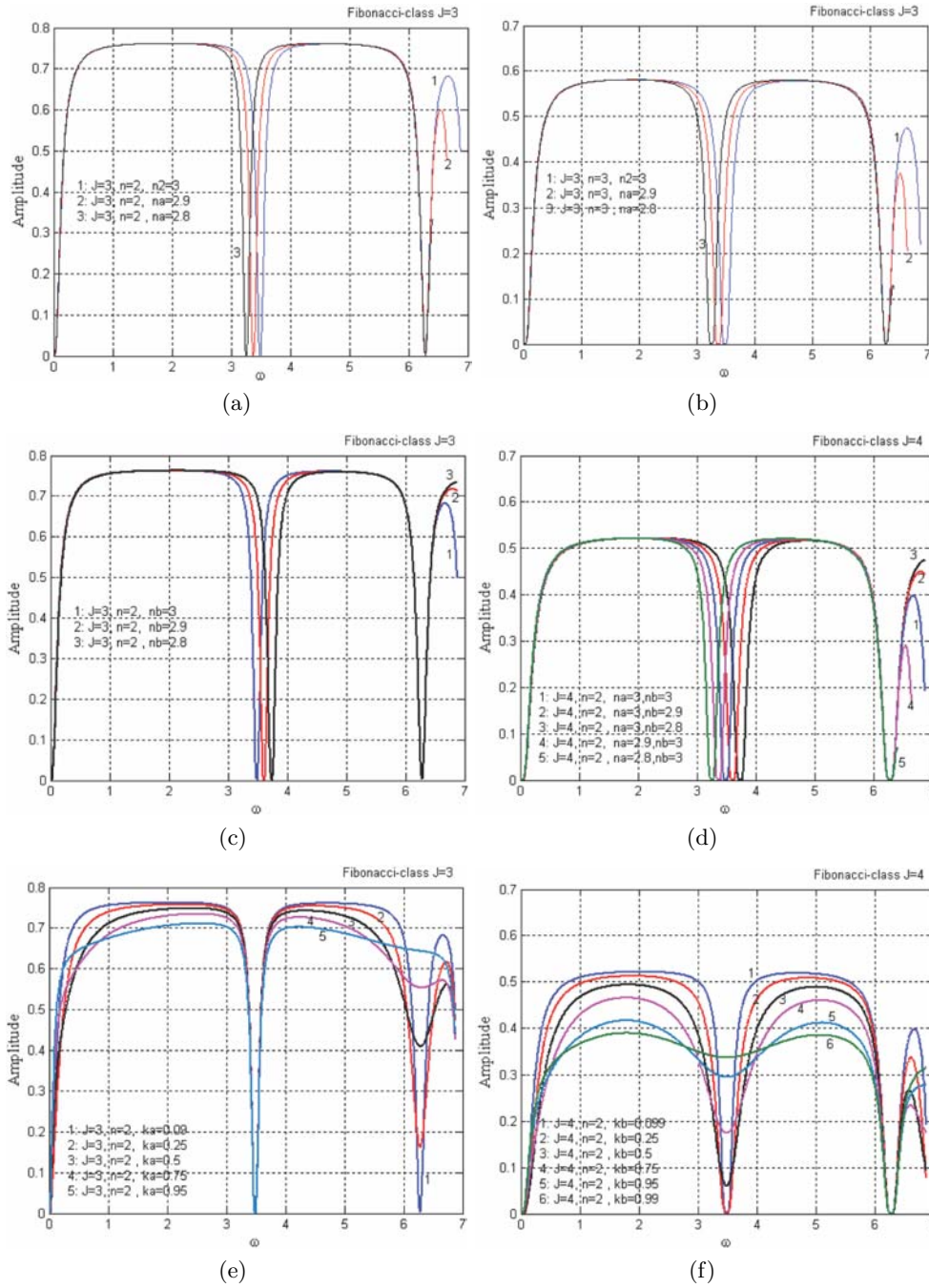


**Fig. 6.** (a) Transmission coefficients for multi-band operation (for  $J = 3$ ,  $n = 2$  and  $n_a = 3, 2.9, 2.8$ ) vs. phase ( $0 - 2\pi$  for  $1.55 \mu\text{m}$ ) ( $\lambda = 1.55 \mu\text{m}$ ,  $L = 20 \mu\text{m}$ ,  $n_0 = 1.5$ ,  $\alpha_a = \alpha_b = \alpha_0 = 5 \times 10^{-5} (\mu\text{m})^{-1}$ ,  $n_b = 3$ ,  $r_a = 100 \mu\text{m}$ ,  $r_b = 180 \mu\text{m}$ ,  $\gamma_a = \gamma_b = 0.1$ ,  $k_a = 0.09$ ,  $k_b = 0.099$ ). (b) Transmission coefficients for multi-band operation (for  $J = 3$ ,  $n = 3$  and  $n_a = 3, 2.9, 2.8$ ) vs. phase ( $0 - 2\pi$  for  $1.55 \mu\text{m}$ ) ( $\lambda = 1.55 \mu\text{m}$ ,  $L = 20 \mu\text{m}$ ,  $n_0 = 1.5$ ,  $\alpha_a = \alpha_b = \alpha_0 = 5 \times 10^{-5} (\mu\text{m})^{-1}$ ,  $n_b = 3$ ,  $r_a = 100 \mu\text{m}$ ,  $r_b = 180 \mu\text{m}$ ,  $\gamma_a = \gamma_b = 0.1$ ,  $k_a = 0.09$ ,  $k_b = 0.099$ ). (c) Transmission coefficients for multi-band operation (for  $J = 3$ ,  $n = 2$  and  $n_b = 3, 2.9, 2.8$ ) vs. phase ( $0 - 2\pi$  for  $1.55 \mu\text{m}$ ) ( $\lambda = 1.55 \mu\text{m}$ ,  $L = 20 \mu\text{m}$ ,  $n_0 = 1.5$ ,  $\alpha_a = \alpha_b = \alpha_0 = 5 \times 10^{-5} (\mu\text{m})^{-1}$ ,  $n_a = 3$ ,  $r_a = 100 \mu\text{m}$ ,  $r_b = 180 \mu\text{m}$ ,  $\gamma_a = \gamma_b = 0.1$ ,  $k_a = 0.09$ ,  $k_b = 0.099$ ). (d) Transmission coefficients for multi-band operation (for  $J = 4$ ,  $n = 2$  and  $n_a = 3, 2.9, 2.8$  and  $n_b = 3, 2.9, 2.8$ ) vs. phase ( $0 - 2\pi$  for  $1.55 \mu\text{m}$ ) ( $\lambda = 1.55 \mu\text{m}$ ,  $L = 20 \mu\text{m}$ ,  $n_0 = 1.5$ ,  $\alpha_a = \alpha_b = \alpha_0 = 5 \times 10^{-5} (\mu\text{m})^{-1}$ ,  $r_a = 100 \mu\text{m}$ ,  $r_b = 180 \mu\text{m}$ ,  $\gamma_a = \gamma_b = 0.1$ ,  $k_a = 0.09$ ,  $k_b = 0.099$ ). (e) Transmission coefficients for multi-band operation (for  $J = 3$ ,  $n = 2$  and  $k_a = 0.09, 0.25, 0.5, 0.75, 0.95$ ) vs. phase ( $0 - 2\pi$  for  $1.55 \mu\text{m}$ ) ( $\lambda = 1.55 \mu\text{m}$ ,  $L = 20 \mu\text{m}$ ,  $n_0 = 1.5$ ,  $\alpha_a = \alpha_b = \alpha_0 = 5 \times 10^{-5} (\mu\text{m})^{-1}$ ,  $n_a = 3$ ,  $n_b = 3$ ,  $r_a = 100 \mu\text{m}$ ,  $r_b = 180 \mu\text{m}$ ,  $\gamma_a = \gamma_b = 0.1$ ,  $k_b = 0.099$ ). (f) Transmission coefficients for multi-band operation (for  $J = 4$ ,  $n = 2$  and  $k_b = 0.099, 0.25, 0.5, 0.75, 0.95, 0.99$ ) vs. phase ( $0 - 2\pi$  for  $1.55 \mu\text{m}$ ) ( $\lambda = 1.55 \mu\text{m}$ ,  $L = 20 \mu\text{m}$ ,  $n_0 = 1.5$ ,  $\alpha_a = \alpha_b = \alpha_0 = 5 \times 10^{-5} (\mu\text{m})^{-1}$ ,  $n_a = 3$ ,  $n_b = 3$ ,  $r_a = 100 \mu\text{m}$ ,  $r_b = 180 \mu\text{m}$ ,  $\gamma_a = \gamma_b = 0.1$ ,  $k_a = 0.09$ ).

## 4 Conclusion

Since, the ring resonators can be integrated on semiconductor wafers, any system design with ring resonators can be integrated and this is very excellent advantage. Optical multi-band filters are important for modern signal processing. So in this paper, we have shown that using Fibonacci-class ring resonators the multi-band optical filters can be obtained. Our design has monolithic capability on semiconductors. Also, with simulated parameters, which is given in figures, our designed filters have central wavelength at  $1.55 \mu\text{m}$  and bandwidth less than 0.001 of central wavelength. Of course, bandwidth can be optimized and lower bandwidths can be obtained. The effects of Fibonacci-class ( $J$ ) and generalization factors ( $n$ ) on transmission coefficient are discussed. Also, the system parameters effects on optical filtering operation studied. We have shown that with coupling factors and ring resonator diameters, we can control the system bandwidth, the position and the number of additional bands.

## References

1. X. Yang, Y. Liu, X. FU, Phys. Rev. B **59**, No. 7 (1999)
2. J.D. Joannopolose, R.D. Meade, J.N. Winn, *Photonic Crystals: Modeling the flow of light* (Princeton University Press, 1995)
3. A. Rostami, S. Matloub, Laser Phys. **14**, No. 12 (2004)
4. A. Rostami, S. Matloub, *Multi-band Optical Filter Design Using Fibonacci based Quasi-periodic Homogeneous Structures*, in *Proceeding of the AP-RSC2004*, edited by Qing Dao (China, 2004)
5. X. Yang, Y. Liu, Eur. Phys. J. B **15**, 625 (2000)
6. R. Lifshitz, *Quasicrystals: A Matter of Definition*, in *Foundations of Physics* **33**, No. 12 (2003)
7. A. Rostami, G. Rostami, *All-Optical Implementation of Tunable Low pass, High pass and Band pass Optical filters Using Ring Resonators*, Optics Communication (2004); G. Rostami, A. Rostami, *All-optical Coding System using Nonlinear Ring Resonator*, Laser Phys. Lett. (2004)
8. A. Rostami, G. Rostami, *Full-Optical Analog to Digital (A/D) Converter Using Kerr-like Nonlinear Ring Resonator*, Optics Communications (2003); G. Rostami, A. Rostami, *Design of All-optical Tunable Butterworth High pass Filters Using Ring Resonators and EIT* in *Proceeding of Asia Pacific Communication Conference, APCC2004, Beijing, China, August 2004*; G. Rostami, A. Rostami, *All-optical Pole and Zero Blocks for Implementation of Optical Engineering Systems*, in *Proceeding of Asia Pacific Communication Conference, APCC2004, Beijing, China, August 2004*
9. J.K.S Poon et al., Optics Express **12**, No. 1 (2004)
10. J.E. Heebner, R.W. Boyd, *Strong dispersive and Nonlinear Optical Properties of Micro-resonator-modified Optical Waveguide*, in *Proceeding of SPIE*, **4969** (2003); J.E. Heebner, R.W. Boyd, Phys. Rev. E **65**, (2002); J.E. Heebner, R.W. Boyd, J. Mod. Optics **49**, 2629 (2002); J.K.S. Poon, J. Scheuer, Y. Xu, A. Yariv, J. Opt. Soc. Am. B **21**, No. 9 (2004)